

# A Mechanism for Spatio-Temporal Disorder in Bistable Reaction-Diffusion Systems

Aric Hagberg

Center for Nonlinear Studies and T-7, Theoretical Division,  
Los Alamos National Laboratory, Los Alamos, NM 87545  
(aric@lanl.gov)

Ehud Meron

The Jacob Blaustein Institute for Desert Research and the Physics Department,  
Ben-Gurion University, Sede Boker Campus 84990, Israel  
(ehud@bgumail.bgu.ac.il)

November 1996

The electronic form of this document can be found at <http://www.springer-ny.com/nst/nstarticles.html>

## Abstract

In bistable systems, the stability of front structures often influences the dynamics of extended patterns. We show how the combined effect of an instability to curvature modulations and proximity to a pitchfork front bifurcation leads to spontaneous nucleation of spiral waves along the front. This effect is demonstrated by direct simulations of a FitzHugh-Nagumo (FHN) model and by simulations of order parameter equations for the front velocity and curvature. Spontaneous spiral-wave nucleation often results in a state of spatio-temporal disorder involving repeated events of spiral wave nucleation, domain splitting and spiral wave annihilation.



Figure 1: The evolution of an unstable front solution connecting the up state (black) to the down state (white) in a bistable FHN reaction-diffusion system. The frames, from left to right, represent the pattern solution at successive moments in time. Perturbations on the flat traveling front grow and nucleate spiral pairs along the front line (see the Appendix for a different view of the middle frame). The resulting disordered state is characterized by domain splitting and spiral-wave nucleation and annihilation.

## 1 Introduction

Spatio-temporal disorder is a ubiquitous phenomenon in extended nonequilibrium systems yet the mechanisms responsible for it are only partially explored. A generic mechanism for the onset of disorder in *periodic patterns* consists of phase instabilities followed by the formation of phase singularities which appear as dislocation defects or vortices [1]. This mechanism has been observed in numerical simulations of the complex Ginzburg-Landau equation [2, 3], and in experiments, e.g. electroconvection in liquid crystals [4]. A considerable effort has been devoted to elucidating the nature of the transition from the regular phase regime to the regime where vortices or defects spontaneously appear [5, 6, 7, 8, 9]. Other mechanisms involving instabilities of periodic patterns, leading to spiral breakup, have been reported recently [10, 11, 12, 13].

In this article we present a mechanism for the onset of spatio-temporal disorder associated with *front structures*. This type of disorder is illustrated by a numerical solution of a bistable FitzHugh Nagumo (FHN) type reaction-diffusion system (Fig. 1). An almost flat front, connecting the two stable uniform stationary states, begins traveling through the system. The front represents an “up” state (black) invading a “down” state (white). Initial nonuniform perturbations of the front position grow into wiggles which nucleate pairs of spiral waves (see the Appendix for a different view of the middle frame in Fig. 1.) The solution then evolves into a disordered state with repeated events of domain splitting and spiral-wave nucleation and annihilation. Similar phenomena have been observed in experiments on the ferrocyanide-iodate-sulfite (FIS) reaction [14, 15].

## 2 The NIB front bifurcation and spontaneous front reversals

The key to understanding the disorder associated with front structures is a pitchfork bifurcation in the velocity of a propagating front. The front bifurcation is represented by the equation

$$C^3 - (\lambda_c - \lambda)C = 0, \quad (1)$$

where  $C$  is the velocity of a flat front and  $\lambda$  is a control parameter. The corresponding bifurcation diagram is shown in Fig. 2. A stationary front ( $C = 0$ ) becomes unstable below a critical parameter value,  $\lambda = \lambda_c$ . At that point two new stable front solutions appear, representing an up state invading a down state ( $C > 0$ ) and a down state invading an up state ( $C < 0$ ). Hereafter, we refer to these front solutions as to “UD front” and “DU front”, respectively.

This type of front bifurcation has been derived for periodically forced oscillatory systems [16] and for bistable FHN type models [17, 18, 19]. Experimental observations of front bifurcations, or supporting evidence for their existence, have been reported in Refs. [20, 21] for liquid crystals, and in Refs. [22, 23] for chemical reactions. The stationary and counter-propagating fronts are sometimes referred to as Ising

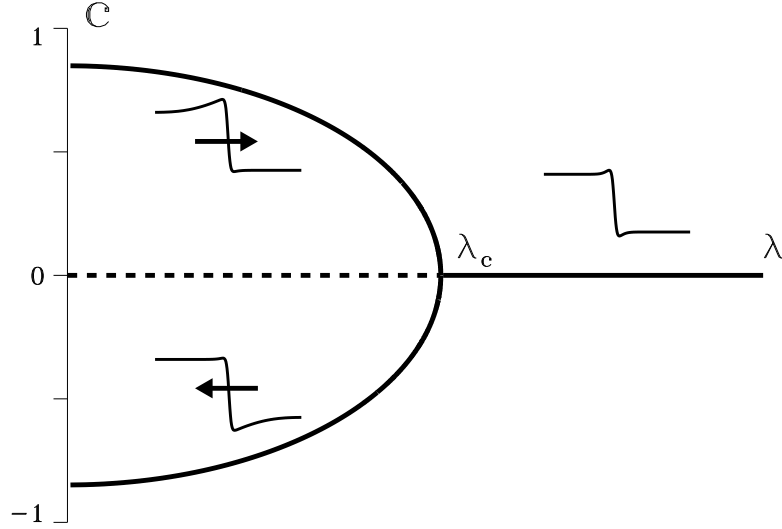


Figure 2: The pitchfork front bifurcation. At  $\lambda = \lambda_c$  the stationary ( $C = 0$ ) front solution becomes unstable to a pair of counterpropagating travelling fronts.

and Bloch fronts, respectively, and the bifurcation itself as a nonequilibrium Ising-Bloch (NIB) bifurcation [16, 18].

Physical realizations of front bifurcations usually involve perturbations that unfold the pitchfork form of (1) into [24]

$$C^3 - (\lambda_c - \lambda)C + \nu_1 + \nu_2 C^2 = 0. \quad (2)$$

An asymmetry between the up and down states is an example of such a perturbation. In the following we confine ourselves to the case  $\nu_2 = 0$ . A plot of the surface (2) in the space spanned by  $C$ ,  $\lambda$  and  $\nu_1$  is shown in Fig. 3. The significance of small variations of  $\nu_1$  in the vicinity of the pitchfork bifurcation point,  $\lambda = \lambda_c$ ,  $\nu_1 = 0$ , is now evident: perturbations may induce transitions between the upper and lower sheets and reverse the direction of front propagation. Notice that farther from the bifurcation point the variations of  $\nu_1$  must be larger in order to induce front reversal.

The dynamics of a single flat front may also be changed by slow dynamical processes such as an approach to a boundary, an interaction with another front, or development of curvature. Fig. 4 shows a typical graph of the normal velocity of a front,  $C_n$ , versus its curvature,  $\kappa$ , for fixed  $\lambda$  near the front bifurcation. The figure was obtained using a singular perturbation analysis of an FHN model, assuming slow curvature dynamics with respect to the time scale of front reversal [25]. The hysteretic shape, similar to the graph of  $C$  versus  $\nu_1$  for fixed  $\lambda$  (see Fig. 3), suggests that front reversals can be induced by small curvature perturbations. Since curvature is an intrinsic dynamical variable, reversals of propagation direction occur spontaneously as the curvature of a front changes. Spontaneous front reversals in catalytic reactions on platinum surfaces have indeed been observed for parameters in the vicinity a front bifurcation [22]. Experimental observations of front reversals induced by boundaries have been reported in [23].

Imagine now a flat UD front that is unstable to transverse perturbations (i.e. an instability to curvature perturbations). As the front propagates, alternating segments along the front acquire negative and positive curvatures. For parameters that place the system near the the front bifurcation, where Fig. 4 applies, segments with negative curvature will eventually reverse propagation direction. Such local front reversals involve the creation of transition zones between the counterpropagating UD and DU fronts. These zones form the cores of *rotating spiral waves*.

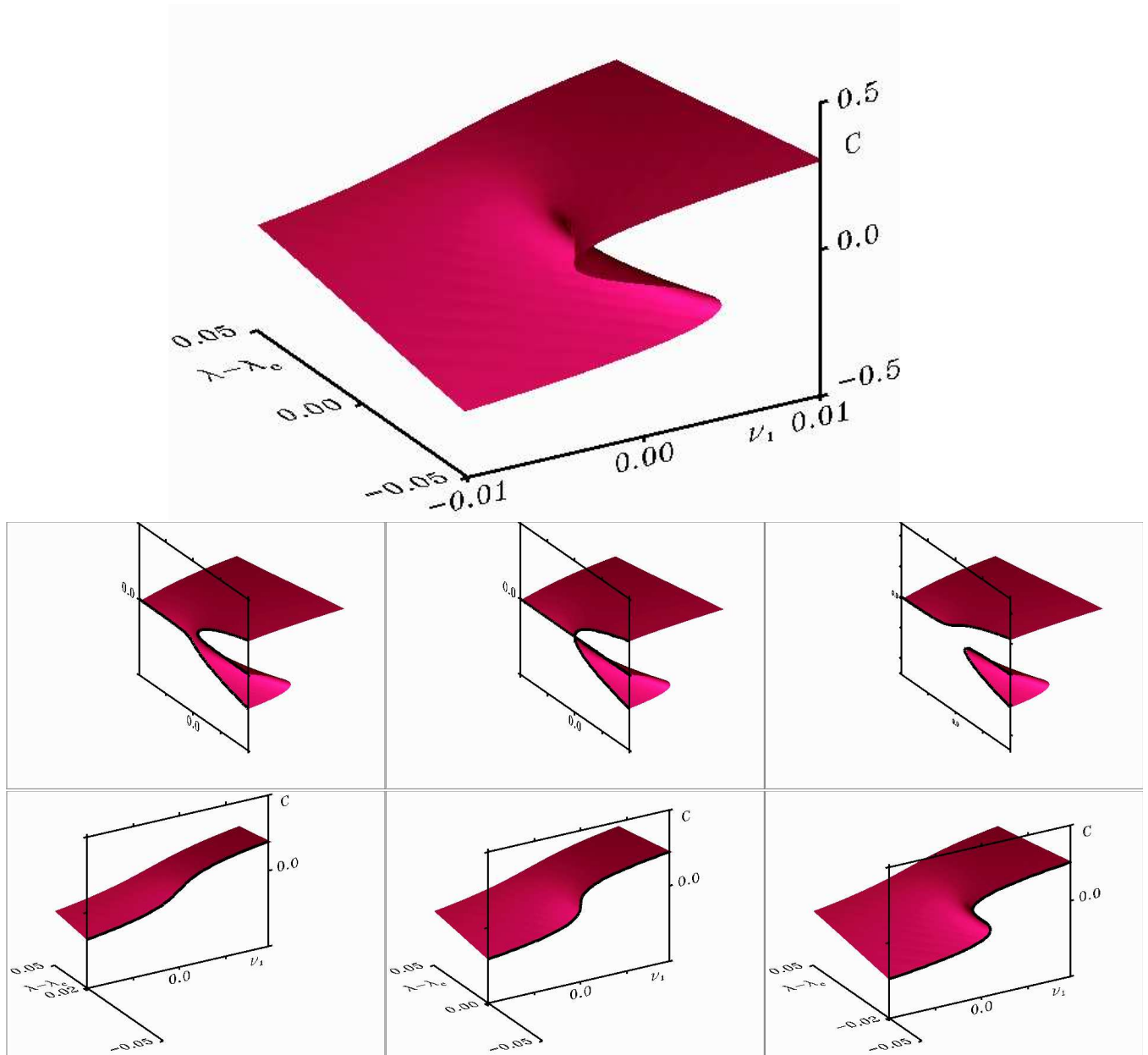


Figure 3: Top: The surface  $C^3 - (\lambda_c - \lambda)C + \nu_1 = 0$  in the space spanned by  $C, \lambda, \nu_1$  (the cusp catastrophe). First triad: A section at  $\nu_1 = 0$  showing the pitchfork bifurcation (center), and sections at  $\nu_1 < 0$  (left) and  $\nu_1 > 0$  (right) showing unfoldings of the pitchfork. Second triad: Sections of the surface at constant  $\lambda$  showing the hysteresis point (center) with single valued (left) and multivalued (right) relations away from the hysteresis point.

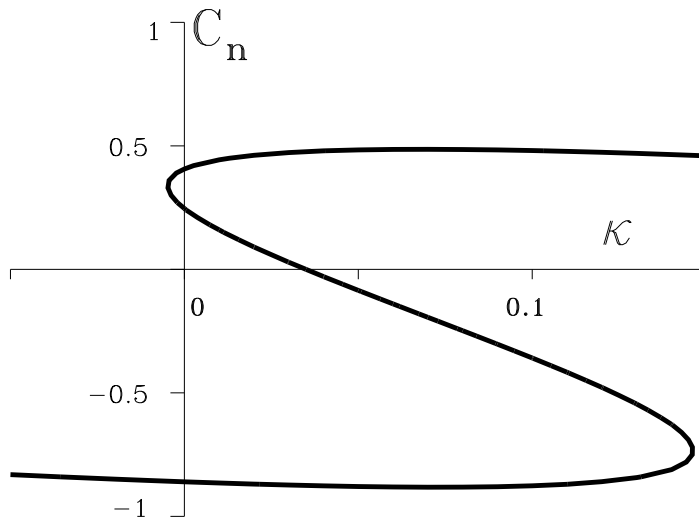


Figure 4: Normal front velocity  $C_n$  vs curvature  $\kappa$  in the vicinity of the front bifurcation. The development of small negative curvature may induce a transition from a UD front ( $C_n > 0$ ) to a DU front ( $C_n < 0$ ).



Figure 5: A closer look at front interactions in the numerical solution of the FHN model from Fig. 1. The repulsive interaction between approaching fronts causes them to reverse direction. The reversal is followed by domain splitting.

The scenario sketched above provides a heuristic explanation for the spontaneous nucleation of spiral waves in Fig. 1 which precedes the onset of spatio-temporal disorder. Similar arguments hold for other intrinsic perturbations such as front interactions. Indeed Fig. 1 includes many events where local front reversals are induced by the interactions between approaching domains. An example of such an event is shown in Fig. 5. Similar processes have been observed in experiments (Figure 6) on the FIS reaction [14, 15].

### 3 The dynamics of front reversals

Algebraic relations like that displayed in Fig. 4 are useful for predicting the onset of spiral-wave nucleation: nucleation events become feasible when a single valued relation becomes multivalued (or hysteretic). Such relations do not, however, contain information about the nucleation process itself. To study the nucleation process a time-dependent approach for the front dynamics is needed. Near the bifurcation, the asymptotic front dynamics are governed by both a translational degree of freedom and an order parameter associated with the bifurcation: the front velocity  $C$ . In Refs. [26, 27] we derived asymptotic dynamic equations for a



Figure 6: Patterns in the Ferrocyanide-Iodate-Sulfite reaction show interactions leading to front reversals followed by domain splittings. These images are from experiments performed in the Center for Nonlinear Dynamics at the University of Texas at Austin.

single unperturbed one-dimensional front using FHN type models. The equations for the front position,  $X$ , and velocity are

$$\begin{aligned}\dot{X} &= C, \\ \dot{C} &= (\alpha_c - \alpha)C - \beta C^3.\end{aligned}\tag{3}$$

These uncoupled equations describe the convergence to constant speed motion Ising (zero speed) and Bloch fronts. Order parameter equations for front propagation in one space dimension near a NIB bifurcation have also been derived in Ref. [28] to study the effects of external fixed heterogeneities.

The effect of curvature is to couple the two equations in a way that allows for front reversal. The equations for the dynamics of a single two-dimensional front with smooth curvature,  $\kappa$ , are [29]

$$\frac{\partial \kappa}{\partial t} = -(\kappa^2 + \frac{\partial^2}{\partial s^2})C_n - \frac{\partial \kappa}{\partial s} \int_0^s \kappa C_n ds',\tag{4}$$

and

$$\frac{\partial C}{\partial t} = (\alpha_c - \alpha)C - \beta C^3 + \gamma \kappa + \gamma_0 + \frac{\partial^2 C}{\partial s^2} - \frac{\partial C}{\partial s} \int_0^s \kappa C_n ds',\tag{5}$$

where  $C_n$ , the normal front velocity, is given by

$$C_n = C - D\kappa,\tag{6}$$

and  $s$  is the arclength coordinate along the front. In deriving these equations an asymmetry between the up and down states has been introduced. Equation (4), for the curvature of the front, follows from purely geometric considerations [30, 31]. Equation (5), for the speed of the front, is valid near the front bifurcation and the boundary of instability to transverse perturbations [25, 29]. The integral term in both equations represents “advection” of changes in  $C$  and  $\kappa$  from the stretching of the arclength over time. Note that away from the front bifurcation where the time scale associated with front reversal,  $(\alpha_c - \alpha)^{-1}$ , is short,  $C$  is no longer a slow variable and can be eliminated adiabatically. For a circular front, equation (5) then reduces to an algebraic relation between the normal front velocity and its curvature such as the one in Fig. 4.

We have computed numerical solutions of equations (4) and (5) starting with an almost flat UD front as an initial condition. Fig. 7 pertains to parameter values in the Bloch regime where the UD and DU fronts coexist and are both stable to transverse perturbations. The initial front converges to a flat UD front propagating at constant speed. Crossing the transverse instability boundary causes perturbations on the front to grow. Near the NIB bifurcation, the growing curvature triggers the “nucleation” of a front segment with opposite velocity as shown in Fig. 8. The front structures in the  $C$ - $s$  plane, separating segments with positive and negative velocities, pertain to spiral waves in the physical two-dimensional plane.

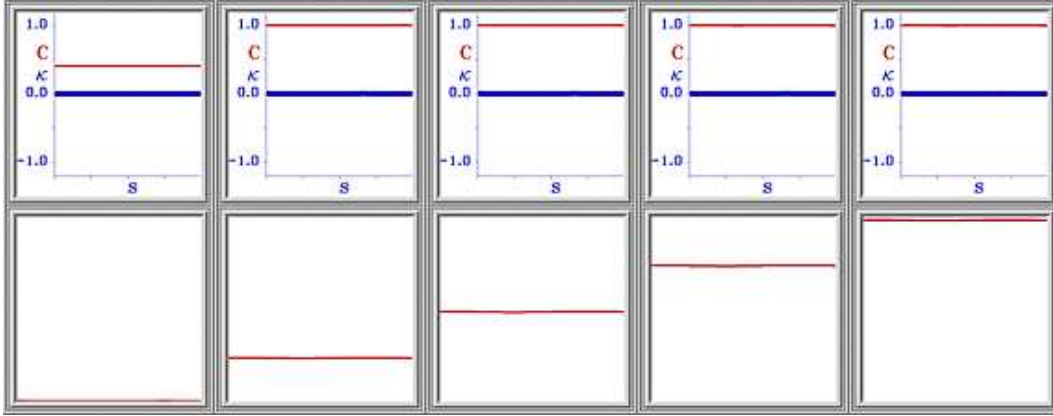


Figure 7: A solution to equations (4) and (5) when the two-dimensional front is stable to transverse perturbations. The frames in the top row show the time evolution of  $C(s)$  (thin line) and  $\kappa(s)$  (thick line). The solution converges to a constant speed flat ( $\kappa = 0$ ) traveling front. The frames in the bottom row display the corresponding dynamics of the front in the physical two-dimensional plane.

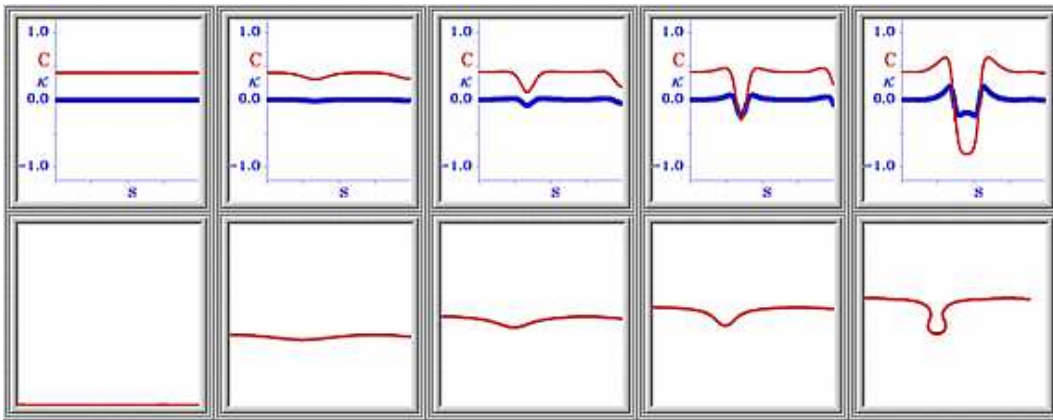


Figure 8: A solution to equations (4) and (5) when the two-dimensional front is unstable to transverse perturbations. The frames in the top row show the evolution of  $C(s)$  (thin line) and  $\kappa(s)$  (thick line). The frames in the bottom row display the corresponding dynamics of the front line in the physical two-dimensional plane. A small curvature perturbation grows and the negative curvature triggers the formation of a region where the front speed becomes negative. The boundary points of this region form the cores of new rotating spiral waves.

## 4 Conclusion

We have presented a new mechanism for spontaneous spiral-wave nucleation in bistable media that leads to spatio-temporal disorder. Unlike most other mechanisms which involve destabilization of periodic patterns (see however [32, 33]), this mechanism involves destabilization of *fronts* and may induce spatio-temporal disorder from a single front state. The dynamical equations, (4) and (5), for the front speed and curvature, describe the asymptotic behavior of fronts near the front bifurcation and the transverse instabilities. These equations capture the process of spiral-wave nucleation and can be used to analyze the transition from the stable curvature dynamics shown in Fig. 7 to dynamics involving nucleation events shown in Fig. 8. It would be interesting to find if an intermediate parameter range exists where the curvature fluctuates but no nucleation events occur.

## 5 Appendix

The model used to demonstrate the nucleation of spiral-vortices in Fig. 1 is a doubly-diffusive version of the FitzHugh-Nagumo Equations

$$\begin{aligned}u_t &= \epsilon^{-1}(u - u^3 - v) + \delta^{-1}u_{xx}, \\v_t &= u - a_1v - a_0 + v_{xx}.\end{aligned}$$

The parameters  $a_0$  and  $a_1$  are chosen such that the equations have two stable uniform solutions (bistable) and  $\epsilon$  and  $\delta$  control the type and stability of front solutions between those two stable states.

Fig. 9 shows a closeup of the middle frame in Fig. 1. The transverse instability of the original front solution has already caused the formation of spiral-vortex pairs along the front. The spiral-vortices are identified with the crossing points of the zero contour lines of the  $u$  and  $v$  fields. At these points the normal front velocity is zero. On either side of the spiral-vortex the front propagates in opposite directions.

## References

- [1] P. Couillet, L. Gil, and J. Lega, *Physica D* **37**, 91 (1989).
- [2] P. Couillet, L. Gil, and J. Lega, *Phys. Rev. Lett.* **62**, 1619 (1989).
- [3] T. Bohr, T. Pedersen, and A. W. Jensen, *Phys. Rev. A* **42**, 3626 (1990).
- [4] I. Rehberg, S. Rasenat, and V. Steinberg, *Phys. Rev. Lett.* **62**, 756 (1989).
- [5] B. I. Shraiman, A. Pumir, W. van Saarloos, P. C. Hohenberg, H. Chate, and M. Holen, *Physica D* **57**, 241 (1992).
- [6] H. S. Greenside and D. A. Egolf, *Phys. Rev. Lett.* **74**, 1751 (1995).
- [7] G. D. Granzow and H. Riecke, *Phys. Rev. Lett.* **77**, 2451 (1996).
- [8] P. Manneville and H. Chate, *Physica D* **96**, 30 (1996).
- [9] H. Chate and P. Manneville, *Physica A* **224**, 348 (1996).
- [10] M. Courtemanche and A. T. Winfree, *Int. J. Bifurcation Chaos* **1**, 431 (1991).
- [11] A. V. Holden and A. V. Panfilov, *Int. J. Bifurcation Chaos* **1**, 219 (1991).
- [12] A. Karma, *Phys. Rev. Lett.* **71**, 1103 (1993).



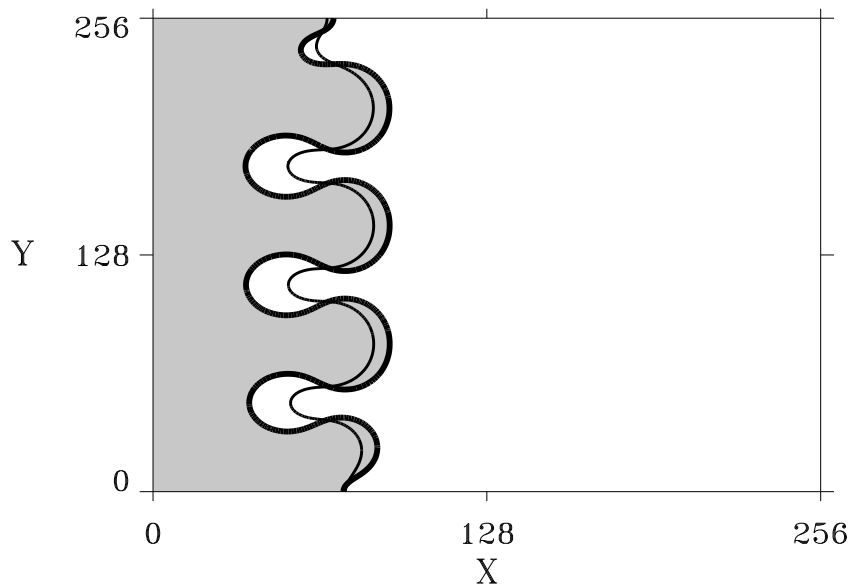


Figure 9: Nucleation of spiral-vortex pairs in the FHN model. Each crossing of the zero contour lines of the  $u$  field (thick line) and  $v$  field (thin line) represents a spiral-vortex that forms the core of a rotating spiral wave.

- [13] M. Bär and M. Eiswirth, *Phys. Rev. E* **48**, R1635 (1993).
- [14] K. J. Lee, W. D. McCormick, J. E. Pearson, and H. L. Swinney, *Nature* **369**, 215 (1994).
- [15] K. J. Lee and H. L. Swinney, *Phys. Rev. E* **51**, 1899 (1995).
- [16] P. Couillet, J. Lega, B. Houchmanzadeh, and J. Lajzerowicz, *Phys. Rev. Lett.* **65**, 1352 (1990).
- [17] H. Ikeda, M. Mimura, and Y. Nishiura, *Nonlinear Analysis-Theory Methods and Applications* **13**, 507 (1989).
- [18] A. Hagberg and E. Meron, *Nonlinearity* **7**, 805 (1994).
- [19] M. Bode, A. Reuter, R. Schmeling, and H.-G. Purwins, *Phys. Lett. A* **185**, 70 (1994).
- [20] T. Frisch, S. Rica, P. Couillet, and J. M. Gilli, *Phys. Rev. Lett.* **72**, 1471 (1994).
- [21] S. Nasuno, N. Yoshimo, and S. Kai, *Phys. Rev. E* **51**, 1598 (1995).
- [22] G. Haas, M. Bär, I. G. Kevrekidis, P. B. Rasmussen, H.-H. Rotermund, and G. Ertl, *Phys. Rev. Lett.* **75**, 3560 (1995).
- [23] D. Haim, G. Li, Q. Ouyang, W. D. McCormick, H. L. Swinney, A. Hagberg, and E. Meron, *Phys. Rev. Lett.* **77**, 190 (1996).
- [24] M. Golubitsky and D. A. Schaeffer, *Singularities and Groups in Bifurcation Theory* (Springer-Verlag, Berlin, 1985).
- [25] A. Hagberg and E. Meron, *Chaos* **4**, 477 (1994).
- [26] C. Elphick, A. Hagberg, and E. Meron, *Phys. Rev. E* **51**, 3052 (1995).

- [27] A. Hagberg, E. Meron, I. Rubinstein, and B. Zaltzman, *Phys. Rev. Lett.* **76**, 427 (1996).
- [28] M. Bode, *Physica D* **106**, 270 (1997).
- [29] A. Hagberg and E. Meron, *Phys. Rev. Lett.* **78**, 1166 (1997).
- [30] A. S. Mikhailov, *Foundation of Synergetics I: Distributed Active Systems* (Springer-Verlag, Berlin, 1990).
- [31] E. Meron, *Phys. Rep.* **218**, 1 (1992).
- [32] M. Bär, M. Hildebrand, M. Eiswirth, M. Falcke, H. Engel, and M. Neufeld, *Chaos* **4**, 499 (1994).
- [33] J. H. Merkin, V. Petrov, S. K. Scott, and K. Showalter, *Phys. Rev. Lett.* **76**, 546 (1996).